Hindawi
Advances in Meteorology
Volume 2019, Article ID 9240568, 11 pages
https://doi.org/10.1155/2019/9240568

Research Article

Sensitivity of CO_2 and CH_4 Annual Cycles to Different Meteorological Variables at a Rural Site in Northern Spain

Isidro A. Pérez, M. Luisa Sánchez, M. Ángeles García, and Nuria Pardo

Department of Applied Physics, Faculty of Sciences, University of Valladolid, Paseo de Belén 7, 47011 Valladolid, Spain

Correspondence should be addressed to Isidro A. Pérez; iaperez@fa1.uva.es

Received 6 September 2018; Revised 12 December 2018; Accepted 19 January 2019; Published 6 February 2019

Academic Editor: Panagiotis Nastos

The focus of the current paper is to explore the influence of meteorological variables on atmospheric CO_2 and CH_4 mean annual cycles at a rural site. Four variables were investigated: boundary layer height, recirculation factor, trajectory direction, and wind speed modelled at the altitude of the site. Boundary layer height and wind speed were provided by the METeorological data EXplorer (METEX) model. Recirculation factor and trajectory direction were obtained from calculations based on this trajectory model, and a nonparametric procedure was used to obtain a smooth evolution. The main results are higher concentrations obtained during the night, attributed to lower dispersion in this period. The smoothed values of the boundary layer height reached nearly 1200 m AGL during the day in August, and its low values caused high concentrations in spring. During the night, the recirculation factor and wind speed showed a sharp contrast between summer and winter. The average recirculation factor was low, 0.10, and average wind speed was 5.1 $m \cdot s^{-1}$. Trajectories were directionally distributed in four quadrants. Different tests were performed by selecting values of meteorological variables above or below certain thresholds. The influence of these variables reached values around 6.3 and 0.023 ppm for CO_2 and CH_4 average concentrations, respectively, during the day when the boundary layer was below 400 m. The main conclusion of this study is that the influence of meteorological variables should not be ignored. In particular, extremely low boundary layer heights may have noticeable effects on both gases.

1. Introduction

CO_2 and CH_4 are directly linked to climate change, are considered as trace gases in unpolluted environments, and are produced by natural sources at these sites. The contribution of water bodies to these gases is the target of intensive current research [1, 2]. In addition to emissions, their concentrations in the low atmosphere are determined by transport from sources such as populated regions [3], sinks such as vegetation, and soils [4], as well as dispersion in the low atmosphere.

The current paper focuses on the annual evolution of CO_2 and CH_4 measured in Valladolid (Spain), in southwestern Europe, a continent where research on said behaviour in both gases remains scarce [5]. Since the site is located in a rural area, anthropogenic influence is considered to be limited, allowing us to analyse the influence of certain atmospheric variables (boundary layer height, recirculation factor, air mass trajectory, and wind speed) on the concentrations of the two gases.

One key feature is that previous studies have investigated the daily cycle [6, 7]. Once this evolution is known, the current analysis considers the annual cycle. Different analyses reveal that it strongly depends on the site. This annual cycle is affected by a variety of parameters, the specific contribution of each proving rather difficult to distinguish.

When investigating the annual evolution, additional problems are the fast oscillations that hide this cycle. These oscillations may extend over several days and are produced by fronts that sweep the measurement site or the evolution of weather systems. One procedure which can be applied in order to minimize their impact is to use a polynomial fit [8]. However, the main disadvantage of this method is the gap which appears at the edge of the cycle. In the context of the present analysis, fast oscillations are filtered using a kernel function which, moreover, avoids this concentration gap. Another issue to be addressed in the analysis is the noticeable contribution of vegetation (photosynthesis uptake in the daytime and respiration at nighttime) to CO_2, which

suggests that the annual cycle should be split into daytime and nighttime periods.

Air parcel trajectory models are useful tools to investigate the influence of large-scale atmospheric circulation, not only on chemicals but also on local-scale meteorological processes or even living beings [9]. Moreover, trajectory analysis provides information concerning the contribution of local-scale processes with respect to long-range transport [10].

In the current paper, an air trajectory model is used for a twofold purpose. First, the model's outputs are exploited to compute the locations of the air parcel travelling to the measurement site. These locations allow the trajectory direction and air recirculation to be calculated, a topic thus far scarcely investigated. Second, the air trajectory model provides meteorological variables, such as the boundary layer height and wind speed, which are not measured at the site.

The boundary layer height depends on thermodynamic and dynamic mechanisms, in addition to the latitude of the site [11]. The relationship between pollutant concentration and this variable has occasionally been considered. Lai [12] studied air quality in Banqiao, Taiwan, together with different meteorological variables and observed that the boundary layer height was nearly 400 m lower at $PM_{2.5}$ events than at low $PM_{2.5}$ level days. Moreover, low boundary layer height at night led to relatively high polycyclic aromatic hydrocarbon concentrations in Guangzhou City, South China [13]. By contrast, the daily evolution of the boundary layer may be inhibited by intensive transport in the upper levels, as observed in the southwestern Iberian Peninsula during intrusions of Saharan dust, where the dust was confined between 1500 and 5500 m [14].

One section of this paper is devoted to the relationship between CO_2 and CH_4 and the boundary layer height. Pérez et al. [15] analysed CO_2 dilution rates in the atmospheric layer close to the surface by means of temperature and wind speed profiles measured with a sodar equipped with a radioacoustic sounding system (RASS). The range reached by this device was very limited, and the current paper expands this analysis.

Another noticeable topic scarcely investigated to date is air mass recirculation. Coastal areas are suitable sites to analyse the relationship between recirculation and land-sea breeze. Levy et al. [16] considered seven sites in Israel during the period 2000–2004 and proposed a procedure to differentiate between synoptic scale, mesoscale, and local scales based on the mean and standard deviation of wind recirculation between sites. Surkova [17] used different stations on the northern coast of the Black Sea and concluded that recirculation is active in the least ventilated areas where wind speed was low. Breeze circulation was enhanced by relief, which was also responsible for the low impact of the large-scale atmospheric flow. Moreover, the author presented three periods of long-term changes in recirculation between 1900 and 2000, the most rapid increase occurring in the final quarter of the century. However, Papanastasiou and Melas [18] investigated sea breeze in the Volos area, Greece, and concluded that recirculation is not a specific factor of sea breeze days.

The relationship between recirculation and concentration has occasionally been studied. Pérez et al. [19] considered the critical values suggested by Allwine and Whiteman [20] for the wind run and the recirculation factor and found that CO_2 concentration for recirculation was intermediate between concentration for ventilation and stagnation. Pérez et al. [21] calculated one trajectory each night from 20 to 5.30 GMT reaching the same site as the current paper, with CO_2 concentration at 6 GMT being attributed to each trajectory. 200 back trajectories were considered to show two sources of noticeable impact: the first being the influence of recirculation in distances below 100 km and the second, the city of Valladolid. Pérez et al. [22] analysed the recirculation factor in the period 2004–2011 on the east coast of Gran Canaria Island, around 250 km from NW Africa, and concluded that high values showed an annual pattern, reaching their maximum in winter. Air pollutant accumulation and marked impact on air quality were favoured during these events. However, Karagiannidis et al. [23] did not find any successful relationship between the air quality described by the concentration of different pollutants and several meteorological parameters, in particular the recirculation factor, for winter and summer at two measuring stations in Patras, Greece, for the period 2008–2011. Another section of the current paper analyses the influence of recirculation on the CO_2 and CH_4 concentrations measured.

Directional analyses have proved useful for identifying pollution sources. Pérez et al. [24] obtained the histogram for CO_2 concentrations above the 95^{th} percentile to determine sources affecting the measurement site. Ashbaugh et al. [25] used conditional probability to determine the location of major pollutant sources. This probability was calculated by the relationship between the number of observations above a specific concentration, called the truncation level, and the total number of observations, both in a single wind sector. This procedure was used by Pérez et al. [26] to gain insights into CO_2 concentration persistence. Finally, Donnelly et al. [27] used a directional analysis to investigate the influence of air masses on NO_2 concentration at three sites in Ireland. Exploring the relationship between trajectory direction and concentrations of CO_2 and CH_4 is a further objective of the current paper.

Finally, the relationship between these concentrations and wind speed has scarcely been addressed to date. One example is the analysis by García et al. [28], which presented the relationship between CO_2 and wind speed on semihourly means over a one-and-a-half-year period using an exponential function. The rest of this study considers the response of the annual cycle of both trace gases to changes in wind speed.

2. Materials and Methods

2.1. Experimental Description. CO_2 and CH_4 dry concentration was measured with a Picarro G1301 located at the Low Atmosphere Research Centre (CIBA) (41°48′50.25″N, 4°55′58.56″W; 850 m ASL) in Valladolid, Spain. The site is flat and surrounded by nonirrigated crops, with grass being

the main vegetation. Commencing on 15 October 2010, the measuring campaign lasted three years. A noticeable gap in available observations was present in August 2013. This analyser was equipped with a valve sequencer to obtain measurements at three levels: 1.8, 3.7, and 8.3 m, although only the latter was used in this study. Observations lasted 10 min at each level. Around 30 values were sampled per minute, and the first 20 observations were discarded to avoid discontinuities when the level changed.

Calibrations were made every two weeks using three NOAA standards [29], and the concentration was corrected slightly using linear equations calculated from the calibrations.

Air mass trajectories and meteorological variables one-day prior to the arrival at the measuring site were provided by the METEX model [30]. The main features are its flexibility and ease-of-use. Calculations were made with a web-based version. Input requirements were date, interval between initializations, trajectory length, coordinates, and altitude of the site where the trajectory begins or ends, trajectory type (forward or backward), and model type. The kinematic model, selected in this paper, considers the trajectory dominated by the wind velocity components. However, the isentropic model employs an air parcel moving on isentropic surfaces.

Each trajectory's coordinates were supplied by the model on an hourly basis together with certain meteorological variables, such as potential temperature and pressure although the present study only considers the boundary layer height and wind speed. Hourly averages of concentrations were calculated so as to combine them with variables provided by this model.

The Normalized Difference Vegetation Index (NDVI) was obtained from the MODIS on the TERRA satellite and downloaded from EOSDIS Reverb [31]. Each image corresponded to the MOD13 product, with a 16-day period, for the tile with coordinates h17v04. Values were extracted using the Windows Image Manager and Digital Array Viewer programs for the whole image. Software developed by the authors was used to extract the values for the measurement site and to check the quality control, which is available in the file.

Sunrise and sunset were obtained from the National Geographic Institute [32] for Valladolid (41°39′N, 4°43′W), a city located some 25 km SE of the measuring site.

2.2. Kernel Smoothing. When time or directional observations are handled, oscillations may hide the behaviour of the variable investigated. A moving average is the simplest procedure to filter these oscillations. However, this method poses two main drawbacks: the first is that only a small fraction of observations is involved in calculations, and the second is that the measurements averaged have the same weight. The Kernel smoothing method is a nonparametric procedure that calculates mean values by taking into account the proximity of neighbouring observations.

Average concentration, C, was calculated for each day of the year, t, by means of the following function described by Henry et al. [33] and Donnelly et al. [27]:

$$C(t,h) = \frac{\sum_{i=1}^{n} K\left((t-t_i)/h\right) C_i}{\sum_{i=1}^{n} K\left((t-t_i)/h\right)}, \quad (1)$$

where C_i is the concentration measured at time t_i and h is the window width. Although Silverman [34] proposed a method to obtain this window width, the behaviour of the resulting function for different widths is the best selection procedure. Small values of h are sensitive to short-time fluctuations, whilst large values determine smoothed concentrations. A value of 20 days was used in this paper to retain the essential features of the annual cycle. The Gaussian kernel K is defined as

$$K(x) = (2\pi)^{-1/2} \exp\left(-0.5x^2\right), \quad (2)$$

where $x = (t - t_i)/h$ in equation (1).

Equation (1) was used to smooth global concentrations at noon for variables considered during the day, such as the boundary layer height. It was also used at midnight to obtain values of variables at night, such as wind speed.

2.3. Recirculation Factor. Allwine and Whiteman [20] defined this factor for each 24-hour backward air mass trajectory by

$$R = 1 - \frac{L}{S}, \quad (0 \le R \le 1). \quad (3)$$

Its calculation is illustrated with Figure 1. L is the resulting transport distance, the distance between the beginning (24 h) and the end (0 h) of the trajectory, and S is the wind run, the addition of the distances between pairs of consecutive trajectory points:

$$S = \sum_{i=1}^{24} S_i. \quad (4)$$

L and S_i may be calculated by the Sinnott equation [35]:

$$\sin\left(\frac{c}{2}\right) = \left\{ \sin^2\left[\frac{\left(\varphi_i - \varphi_j\right)}{2}\right] + \cos\varphi_i \cos\varphi_j \ \sin^2\left[\frac{\left(\lambda_i - \lambda_j\right)}{2}\right] \right\}^{1/2}, \quad (5)$$

where c is the distance between points (λ_i, φ_i) and (λ_j, φ_j), with λ being the longitude and φ being the latitude.

The recirculation factor is calculated for each trajectory, and values obtained during the night were selected for this study.

2.4. Calculation of the Trajectory Direction. Directional calculations aim to determine the source of the concentrations recorded [24]. However, directions obtained at the measurement site may be affected by local flows. An air parcel trajectory may be slightly affected by local features, and its direction is more robust than that obtained at the measurement site.

The centroid (λ_C, φ_C) of each trajectory was calculated by the mean of the trajectory points coordinates. Its

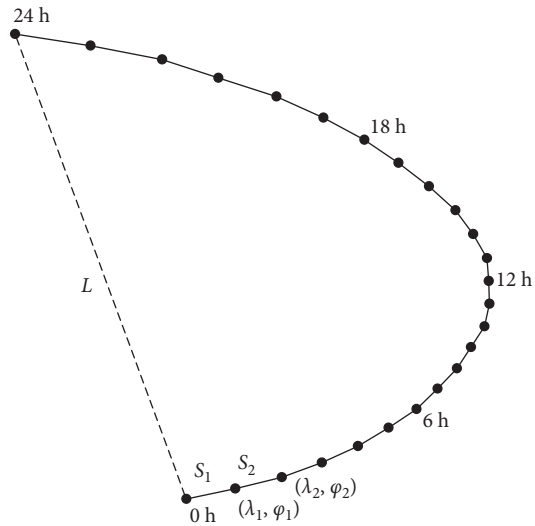

Figure 1: Backward trajectory showing the resulting transport distance L and the distance S_i between pairs of consecutive trajectory points.

direction, d, from the measuring site (λ_0, φ_0) was then obtained by the law of cosines [35]:

$$\cos d = \frac{\cos(90 - \varphi_C) - \cos(90 - \varphi_0)\cos c_C}{\sin(90 - \varphi_0)\sin c_C}, \quad (6)$$

where c_C is the distance between the trajectory centroid and the measurement site, with angles being measured in degrees.

3. Results

3.1. Characteristics of the Diurnal Cycle. Figure 2 presents the annual evolution of both trace gases, and Table 1 presents their corresponding average concentrations calculated from values provided by equation (1) together with their availabilities. The concentration during the day was lower than values observed during the night for both trace gases due to the low dispersion in this period. Noticeable discrepancies between day and night were observed for CO_2 concentration from March to early July, attributed to intense vegetation development, described by the NDVI evolution whose smoothed curve was obtained by applying the Kernel smoothing methodology to the NDVI data provided each 16 days. According to Table 2, values above 0.4 correspond to abundant vegetation. The greatest difference was observed in early May, extending up to about 13 ppm between day and night. CH_4 displayed less contrasting behaviour with day-night differences below 0.010 ppm most of the year. This behaviour was in agreement with the daily cycle presented by García et al. [37] for the same site and two years of measurements.

Regarding the annual evolution, minima were reached in summer for both trace gases. A marked evolution was observed for CO_2 during the night, with a range of 16 ppm between a maximum in early May and a minimum in late August. Consequently, the annual evolution may be divided into two unequal periods: one with a fast decrease in concentration and the other with a slow increase. Another feature is the time difference between nighttime CO_2 and NDVI maxima, which is around half a month, since the NDVI maximum was observed in late May. The CH_4 cycle presented a similar evolution for the three situations. The annual cycle range was around 0.050 ppm between the maximum in winter and the minimum in summer, these being regularly distributed approximately every six months.

The analysis presented in this paper focused on the daytime for the boundary layer height due to the noticeable range of this variable during that period. However, the influence of the remaining variables was considered during the night due to the characteristic CO_2 annual pattern, whose values were considerably higher than those during the day.

3.2. Boundary Layer Height. The METEX model provides the boundary layer heights, the most noticeable changes of this variable being observed during the day. Figure 3 presents the boundary layer evolution smoothed with the Kernel methodology. During winter, its minimum was in December, at about 400 m. However, it increased gradually in winter and at a lower rate in spring and summer, reaching nearly 1200 m in August. After this value, the boundary layer fell sharply during the rest of the year. Its values were similar to that reached at some European sites [38, 39].

Regression analysis between concentration during the day and boundary layer height shown in Figure 3 revealed an inverse relationship between the two variables, with correlation coefficients of 0.919 and 0.974, for CO_2 and CH_4, respectively. This behaviour is in agreement with Pérez et al. [15] and Sreenivas et al. [40]. In summer, plant activity was the lowest and the boundary layer height was greatest, leading to intensive dispersion. By contrast, the boundary layer height was lowest in winter, dispersion was small, and concentration increased due to larger emissions.

Two groups of situations with different thresholds of the boundary layer height were considered to investigate the response of equation (1). The first is formed by evolutions with boundary layer heights above certain thresholds, and the second considers boundary layer heights below the thresholds. An objective procedure for threshold selection was not achieved. Consequently, this should be chosen by taking into account of the frequency of observations and the changes observed in the concentration.

Table 3 presents the frequency of available observations, the number of days without observations (gaps) calculated for annual evolutions, and the differences between the average concentration with different boundary layer heights in 100 m intervals and the average diurnal value. With a high boundary layer height, strong dispersion caused low concentrations. Moreover, when the threshold for large values of the boundary layer increased, the number of available observations decreased. Furthermore, a noticeable gap was observed in autumn and winter when the threshold was above 800 m, since extensive development of the boundary layer is infrequent during this season. The annual evolution

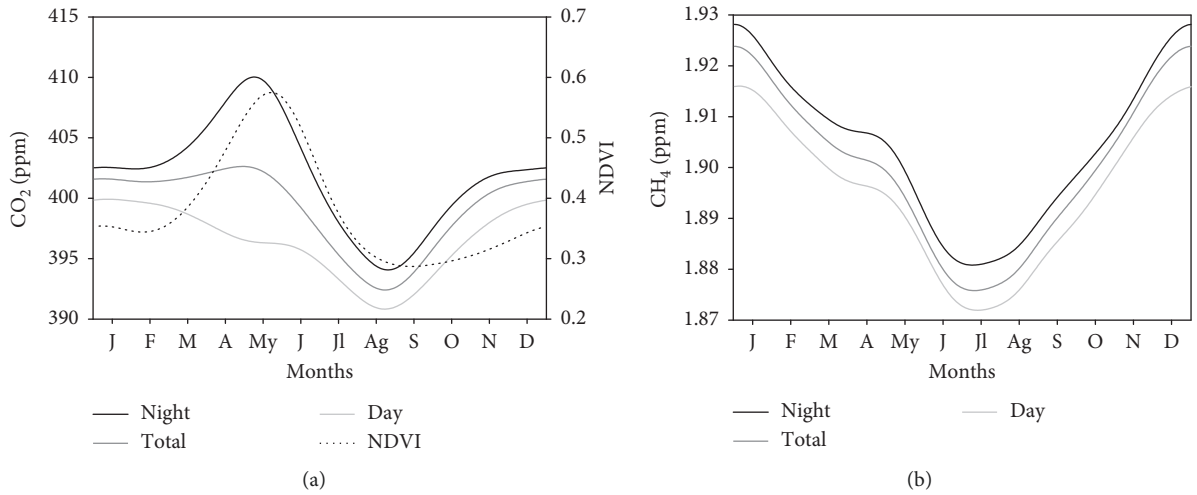

Figure 2: Annual evolution of NDVI and CO_2 (a) and CH_4 (b). Trace gas concentrations have been considered for all the data and for day and night periods.

Table 1: Availabilities and average concentrations calculated with values provided by equation (1).

Period	Availability (%)	CO_2 (ppm)	CH_4 (ppm)
Total	94.9	399.2	1.899
Day	94.0	396.4	1.895
Night	95.6	401.9	1.904

Table 2: Vegetation types following NDVI values*.

NDVI	Vegetation
0–0.2	Bare soil and dead vegetation
0.2–0.4	Shrub or grassland
0.4–0.6	Abundant and vigorous vegetation
>0.6	Very dense and vigorous vegetation

*Provided by the Mapping and Geological Institute of Catalonia [36].

corresponding to this height is presented in Figure 3, whose average concentrations were 2.5 ppm lower for CO_2 and 0.012 ppm lower for CH_4 than those calculated for the diurnal observations. The seasonal pattern in this case was similar to that for diurnal values.

However, for heights below the threshold, concentrations increased. The behaviour of the available observations was the opposite to what emerged when the boundary layer height was above the threshold. In this case, when the threshold increased, the frequency of available values also increased, and a gap was observed in late summer-early autumn when the threshold was below 400 m. The evolutions corresponding to that height are shown in Figure 3. Their corresponding average concentrations increased 6.3 ppm for CO_2 and 0.023 ppm for CH_4. Moreover, a marked seasonal pattern was also observed for CO_2, which may be explained by the daily evolution of the boundary layer height, whose lowest values are reached in early and late daytime. Under these conditions, photosynthesis is low and emissions prevail; hence, the CO_2 maximum was observed in spring when vegetation is developing. This reached up to 13.4 ppm above the corresponding daytime concentration. Finally, similar values were obtained in winter for CO_2 in the three evolutions shown in Figure 3. The seasonal pattern for CH_4 was similar to that for diurnal values.

3.3. Recirculation Factor. The annual evolution of the recirculation factor was calculated using the Kernel smoothing methodology and presented in Figure 4(a). These values were lower than those calculated at different sites presented in Table 4, revealing that marked recirculations are infrequent. Moreover, their range is very narrow since the lowest value, around 0.07, was reached in February and the highest, nearly 0.12, in August.

In order to investigate the recirculation influence on concentrations, two situations were proposed: firstly by considering recirculation factors above certain thresholds (in steps of 0.05) and secondly, below others (in steps of 0.01). Table 5 presents the differences between the average concentration calculated for these situations and those obtained during the night together with their corresponding frequencies of available observations and gaps formed by days without observations.

Concentrations increased together with the recirculation factor for factors above the thresholds. Moreover, the frequency of available observations decreased when the threshold increased. Despite the high number of gaps for the 0.15 threshold, these were uniformly distributed along the year; hence, the small difference was observed in concentrations obtained with the following threshold. Figure 4 presents this evolution, whose concentration was 2.6 ppm higher for CO_2 and 0.012 ppm higher for CH_4 than their corresponding average calculated for nighttime.

CO_2 was mainly affected by high recirculation in March-May and November, with concentrations reaching more than 4 ppm above those calculated with all observations. For CH_4, the greatest difference was observed in late autumn and reached 0.035 ppm.

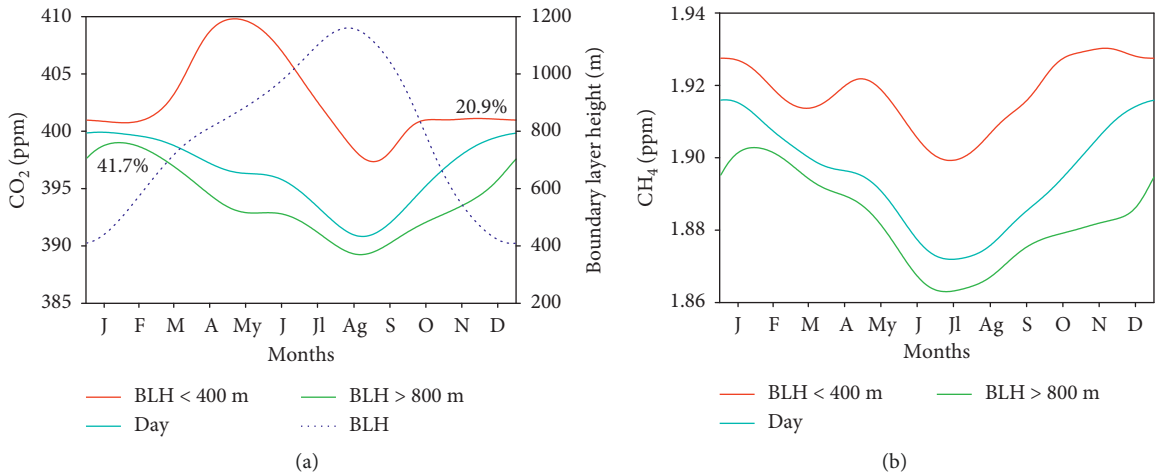

Figure 3: Annual evolution of the boundary layer height (BLH) CO_2 (a) and CH_4 (b) during the day. Three situations were considered: with all the observations (cyan line), for boundary layers below 400 m (red line), and for boundary layer heights above 800 m (green line). The appearance frequency for the low and high boundary layer is also shown.

Table 3: Differences between average concentrations calculated with observations selected for different boundary layer thresholds and the annual cycle for daytime observations. Availabilities and days without observations (gaps) are also included.

Type of test	Boundary layer height threshold (m)	Availability (%)	Gap (days)	CO_2 difference		CH_4 difference	
				ppm	%	ppm	%
Above	500	64.6	15	−1.8	−0.45	−0.009	−0.48
	600	56.8	27	−2.0	−0.51	−0.010	−0.53
	700	48.9	47	−2.2	−0.56	−0.011	−0.58
	800	41.7	72	−2.5	−0.63	−0.012	−0.65
	900	35.1	94	−2.8	−0.70	−0.013	−0.67
	1000	28.5	126	−3.1	−0.79	−0.014	−0.76
Below	300	13	79	7.3	1.85	0.026	1.37
	400	20.9	12	6.3	1.60	0.023	1.22
	500	29.2	1	4.9	1.24	0.018	0.96
	600	37.1	1	3.8	0.97	0.015	0.77
	700	44.9	0	3.0	0.75	0.012	0.61
	800	52.1	0	2.4	0.60	0.009	0.50

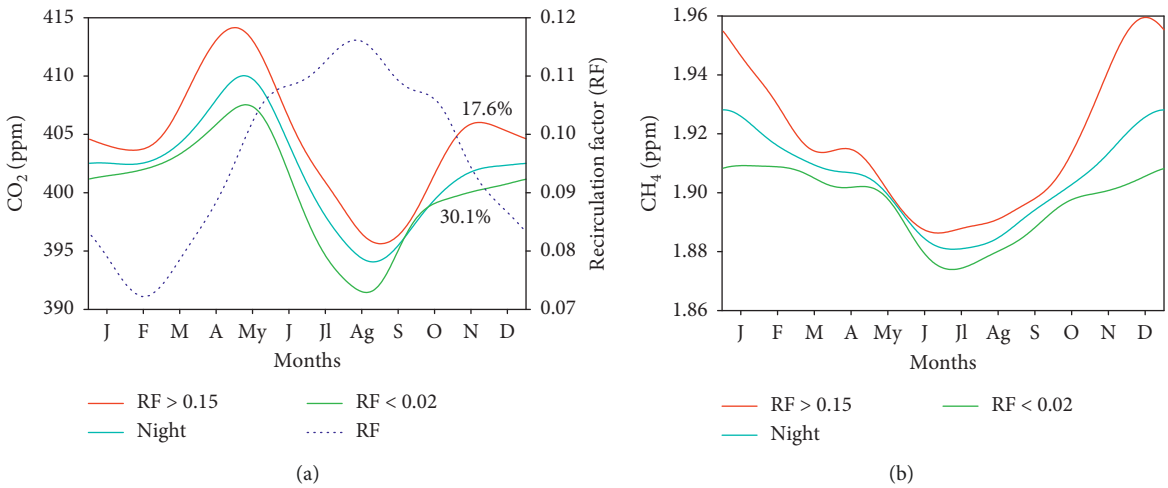

Figure 4: Annual evolution of the recirculation factor (RF) and CO_2 (a) and CH_4 (b) during the night. Three situations were considered: with all the observations (cyan line), for recirculation factors above 0.15 (red line), and for recirculation factors below 0.02 (green line). The appearance frequency for the low and high recirculation factor is also shown.

Table 4: Recirculation factor calculated in different studies.

Site	Recirculation factor (average)	Period (years)	Reference
Portugal	0.10–0.39	9	[41]
India	0.15–0.24	5	[42]
Argentina	0.16–0.25	2	[43]
India	0.21–0.27	6	[44]
Korea	0.23–0.33	2	[45]
Oman	0.26–0.48	5	[46]
Israel	0.27–0.53	5	[47]

High recirculation should determine low dispersion and, consequently, a concentration increase. In this sense, high concentrations are reinforced by recirculation processes, such as in spring for CO_2 and late autumn and early winter for CH_4, added to which intermediate concentrations also grew, in autumn, for both gases.

When observations were selected below the threshold, the frequency of the available observations decreased following the threshold. Observation density was low when the recirculation factor was below 0.02. However, there were few days without observations, and these were uniformly distributed for this threshold. The corresponding annual evolution is presented in Figure 4. Under this condition, average concentrations were less modified than those obtained in the preceding test and were 1.7 ppm below the average for the annual cycle for CO_2 and 0.008 ppm for CH_4.

Minima of evolutions for CO_2 presented in Figure 4 show an advancement of about one week between the cycle for 0.02 threshold and nighttime and between that and the evolution for 0.15 threshold. Moreover, the range for the cycle with the recirculation factor above 0.15 was 18.5 ppm and was greater than the range for the recirculation factor below 0.02, which was 16.1 ppm.

3.4. Trajectory Direction. A detailed analysis of direction does not seem recommendable for one-day trajectory, due to the wind direction change which may be significant for short trajectories. Following Lai [12], four quadrants were considered. Table 6 presents their corresponding availabilities, average wind speeds at the site, and the differences between the average calculated concentrations in the quadrant and for all nighttime observations. In this test, thresholds were not considered since trajectories are distributed in the quadrants. The most frequent sector was NW, with the second highest wind speed, and the least frequent SE, with the lowest wind speed. These frequencies are explained by the synoptic flow affecting the Iberian Peninsula where a western wind prevails [48]. The remaining sectors presented a similar and intermediate frequency. Days without observations, though noticeable for SE, were uniformly distributed, and equation (1) guarantees an accurate calculation.

The most noticeable contrasts were obtained for the directions presented in Figure 5. The average CO_2 concentration for the SE quadrant was 2.5 ppm above the average for all nighttime observations and may be attributed to transport from the city of Valladolid [24]. Moreover, concentration increase in this sector was not uniformly distributed since the greatest differences were obtained from May to July. These differences ranged from 5 to 6 ppm and were probably due to the slow dispersion linked to the low wind speed in this sector [48]. CO_2 concentration was intermediate and similar during autumn and winter. Another noticeable feature with respect to the cycle during the night was the delay observed in the maximum in May and the minimum in September. Differences between the values calculated with all the observations and the low concentration for NE were small for this gas, although they were above 1.5 ppm from March to October. For CH_4, the contrast between sectors was also very small, as shown in Table 6 and Figure 5(b). For this gas, the highest concentration corresponded to NE trajectories and the lowest to NW, with a difference of 0.011 ppm.

3.5. Wind Speed. Wind speed during the night displayed the annual pattern shown in Figure 6. The range is very narrow, around 2.5 $m \cdot s^{-1}$. Large values, around 6 $m \cdot s^{-1}$ were observed in late autumn and winter. However, the lowest wind speed was observed in August, below 4 $m \cdot s^{-1}$. Consequently, its annual cycle evolution is asymmetric, with wind speed decreasing slowly from February to August and increasing sharply from August to November. This result is comparable to evolutions analysed in previous studies such as Lorente-Plazas et al. [49], who presented the annual cycle of wind speed for different regions in the Iberian Peninsula. The annual evolution for central sites is characterised by high values in March but low and similar values during the latter half of the year. However, the cycle obtained was similar to those observed in the north of the peninsula.

Table 7 presents the results of several tests performed with different thresholds of wind speed in steps of 1 $m \cdot s^{-1}$. Figure 6 presents the annual evolution for two selected thresholds in extreme conditions. When wind speeds were above 7 $m \cdot s^{-1}$, a noticeable gap in summer is observed linked with the frequent low wind speeds in this period, and wind speeds below 3 $m \cdot s^{-1}$ led to a low density of observations.

Calculated concentrations were 3.0 and 0.011 ppm lower than those obtained for all observations during the night for CO_2 and CH_4, respectively, when wind speed was above 7 $m \cdot s^{-1}$, indicating that dispersion was favoured under high wind speed. Conversely, calculated concentrations for low wind speeds were higher than those for all observations during the night, reaching 3.4 and 0.013 ppm for CO_2 and CH_4, respectively, when wind speed was below 3 $m \cdot s^{-1}$. These differences may be explained since stagnation conditions prevent dispersion of the two gases.

Several features are observed in the annual evolution. When wind speed was below 3 $m \cdot s^{-1}$, CO_2 was around 5 ppm greater than the corresponding value for the nighttime evolution in late April and early May and a similar amount was lower when wind speed was above 7 $m \cdot s^{-1}$. Moreover, the minimum concentration was nearly one week later with wind speeds below 3 $m \cdot s^{-1}$ compared to the evolution for observations during the night, and it was early by a similar interval for wind speeds above 7 $m \cdot s^{-1}$. The low CO_2

Table 5: Differences between average concentrations calculated with observations selected for thresholds and the annual cycle for nighttime observations. Availability of frequencies and number of days without observations (gaps) are also presented.

Type of test	Recirculation factor threshold	Availability (%)	Gap (days)	CO_2 difference		CH_4 difference	
				ppm	%	ppm	%
Above	0.05	42.9	9	1.4	0.35	0.007	0.36
	0.10	25.9	57	2.2	0.55	0.010	0.51
	0.15	17.6	102	2.6	0.65	0.012	0.62
	0.20	12.7	137	3.1	0.77	0.015	0.76
	0.25	9.5	167	3.3	0.83	0.015	0.81
	0.30	7.5	188	3.8	0.96	0.017	0.92
Below	0.01	17.1	90	−2.2	−0.55	−0.010	−0.51
	0.02	30.1	39	−1.7	−0.41	−0.008	−0.42
	0.03	39.6	17	−1.5	−0.38	−0.007	−0.37
	0.04	47.2	9	−1.4	−0.35	−0.006	−0.33
	0.05	52.7	8	−1.2	−0.31	−0.005	−0.28
	0.06	57.6	7	−1.1	−0.28	−0.005	−0.26

Table 6: Differences between average concentrations calculated for different sectors and from observations during the night, together with their corresponding availabilities, numbers of days without observations (gaps), and average wind speed at the site.

Sector	Availability (%)	Gap (days)	Average wind speed ($m \cdot s^{-1}$)	CO_2 difference		CH_4 difference	
				ppm	%	ppm	%
NE	24.3	100	4.8	−1.3	−0.32	0.006	0.30
SE	13.1	165	4.3	2.5	0.62	0.003	0.16
SW	25.9	76	6.1	0.9	0.22	−0.001	−0.07
NW	32.3	48	5.5	−0.7	−0.18	−0.005	−0.24

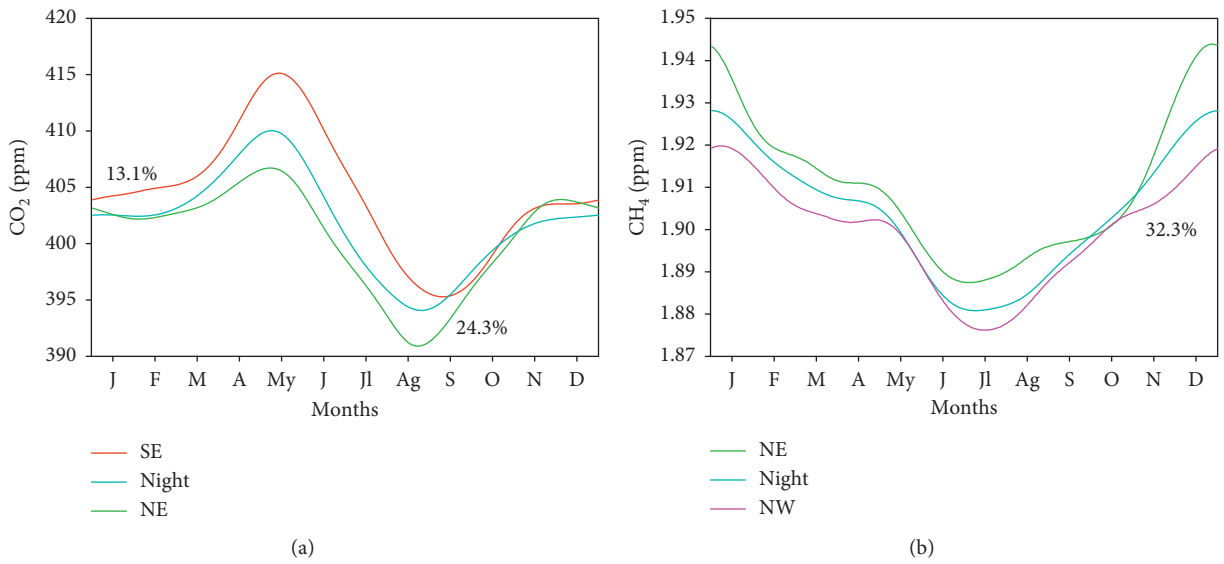

Figure 5: Annual evolution of CO_2 (a) and CH_4 (b) during the night (cyan line) together with the evolution for the trajectory centroid direction of prominent quadrants (red, green, and purple lines). The appearance frequency of each direction is also shown.

concentration in late summer is attributed to the extremely weak plant activity responsible for low emissions. Under this condition, concentration is low despite the low wind speed. CH_4 behaviour was more irregular than CO_2 evolution. Differences between concentrations for wind speeds below 3 $m \cdot s^{-1}$ and those obtained with all the observations were above 0.025 ppm in late autumn and winter. Moreover, the values in January, July, August, and December for wind speed above 7 $m \cdot s^{-1}$ were at least 0.015 ppm lower than those for all values during the night.

4. Conclusions

The key point of the current study is the combination of modelled and measured variables since the influence of meteorological variables on observed CO_2 and CH_4

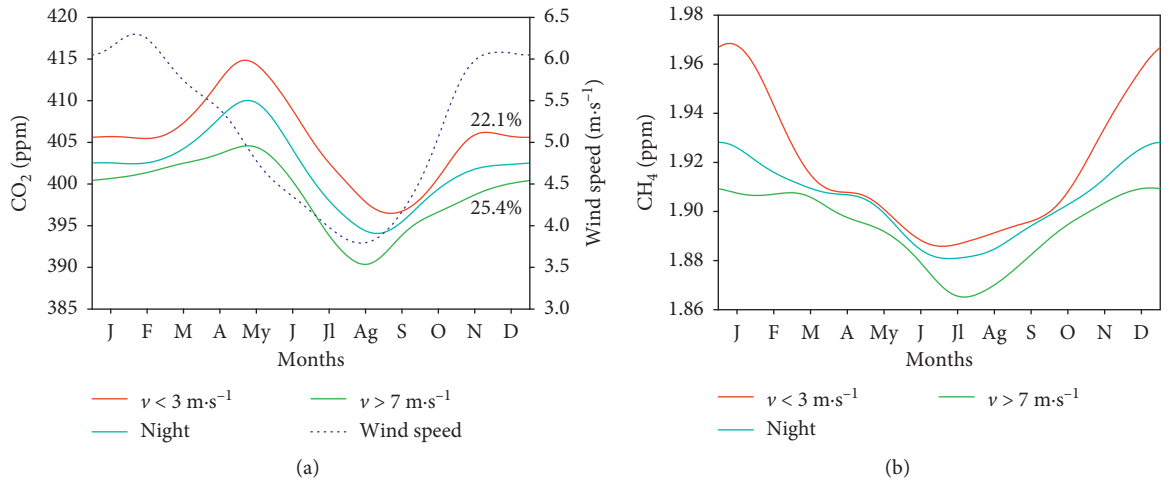

Figure 6: Annual evolution of wind speed and CO_2 (a) and CH_4 (b). Three situations were considered: with all the observations during the night (cyan line), for wind speed below 3 $m \cdot s^{-1}$ (red line), and for wind speed over 7 $m \cdot s^{-1}$ (green line). The appearance frequency for low and high wind is also shown.

Table 7: Differences between average concentrations calculated with observations selected for different thresholds of wind speed and the annual cycle for nighttime observations. Availabilities and numbers of days without observations (gaps) are presented.

Type of test	Wind speed threshold ($m \cdot s^{-1}$)	Availability (%)	Gap (days)	CO_2 difference		CH_4 difference	
				ppm	%	ppm	%
Above	9	11.1	182	−4.4	−1.10	−0.017	−0.91
	8	17.2	130	−3.8	−0.95	−0.014	−0.73
	7	25.4	85	−3.0	−0.75	−0.011	−0.57
	6	35.3	58	−2.7	−0.66	−0.007	−0.38
	5	47.0	20	−2.1	−0.53	−0.005	−0.27
	4	59.6	6	−1.7	−0.41	−0.005	−0.24
Below	2	11.1	136	3.5	0.88	0.013	0.68
	3	22.1	68	3.4	0.85	0.013	0.67
	4	35.9	24	2.5	0.63	0.009	0.47
	5	48.6	7	1.8	0.46	0.006	0.32
	6	60.3	2	1.3	0.33	0.005	0.25
	7	70.2	2	0.9	0.23	0.004	0.21

concentrations is investigated. Prominent among the modelled variables provided by an air parcel trajectory model is boundary layer height, with its impact being quantified, whereas the shape of the trajectories is analysed from the recirculation factor, calculated from the geographical coordinates of such trajectories.

High concentrations during the night were attributed to the low atmospheric dispersion in this period. The sharp contrast between day and night observed in spring for CO_2 was due to intense vegetation growth during this season that strengthened respiration during the night and photosynthesis during the day. Annual CH_4 evolution remained nearly unchanged when only day or night was selected.

The annual pattern of the boundary layer height during the day evolved from 400 m in December-January, to nearly 800 m in March-April and reaching slightly below 1200 m in July-August, favouring dispersion in this period.

Trajectories reaching the measuring site recirculated slightly, and the annual wind speed pattern showed a small fluctuation range, 2.5 $m \cdot s^{-1}$ during the night. Despite their slight evolution, both variables showed opposite cycles since high wind speed is associated with trajectories that have only slight recirculation.

Trajectory direction showed a noticeable contrast since the NW sector was the most frequent, whereas the opposite sector, the SE sector, was the least frequent, in agreement with the synoptic flow affecting the Iberian Peninsula.

The kernel smoothing procedure emerges as a suitable procedure to investigate the response of the concentrations to different thresholds. As a result of the tests performed, a concentration increase was observed under meteorological conditions that inhibited dispersion. Particularly, low values of the boundary layer height were associated with noticeable increases in concentrations. However, slight displacements were observed when recirculation, direction, or wind speed was filtered. Moreover, CH_4 was more robust to tests of meteorological values than CO_2, whose concentration proved more sensitive.

Among the natural processes that determine the annual evolution of CO_2 and CH_4 at this site, meteorological

variables, which have been analysed separately in this paper, may have a noticeable impact on concentrations of both greenhouse gases.

Data Availability

The CO_2 and CH_4 observations used in this study are available from the lead researcher of the project, Prof. M. Luisa Sánchez (marisa@fa1.uva.es), upon request. METEX simulations were made from http://db.cger.nies.go.jp/metex/trajectory.html. NDVI data were downloaded from https://earthdata.nasa.gov/. Sunrise and sunset data were obtained from the National Geographic Institute (http://www.fomento.gob.es/).

Conflicts of Interest

The authors declare there are no conflicts of interest regarding publication of this paper.

Acknowledgments

The authors wish to acknowledge the financial support of the Ministry of Economy and Competitiveness and ERDF funds (projects CGL2009-11979 and CGL2014-53948-P).

References

[1] A. Sepulveda-Jauregui, K. M. Walter Anthony, K. Martinez-Cruz, S. Greene, and F. Thalasso, "Methane and carbon dioxide emissions from 40 lakes along a north-south latitudinal transect in Alaska," *Biogeosciences*, vol. 12, no. 11, pp. 3197–3223, 2015.

[2] C. R. Teodoru, F. C. Nyoni, A. V. Borges, F. Darchambeau, I. Nyambe, and S. Bouillon, "Dynamics of greenhouse gases (CO_2, CH_4, N_2O) along the Zambezi River and major tributaries, and their importance in the riverine carbon budget," *Biogeosciences*, vol. 12, no. 8, pp. 2431–2453, 2015.

[3] F. Zhang, L. Zhou, and L. Xu, "Temporal variation of atmospheric CH_4 and the potential source regions at Waliguan, China," *Science China Earth Sciences*, vol. 56, no. 5, pp. 727–736, 2013.

[4] C.-S. Lee and P.-J. Su, "Tracking sinks of atmospheric methane using small world networks," *Chemosphere*, vol. 117, no. 1, pp. 766–773, 2014.

[5] L. Haszpra, Z. Barcza, D. Hidy, I. Szilágyi, E. Dlugokencky, and P. Tans, "Trends and temporal variations of major greenhouse gases at a rural site in Central Europe," *Atmospheric Environment*, vol. 42, no. 38, pp. 8707–8716, 2008.

[6] M. L. Sánchez, M. Á. García, I. A. Pérez, and N. Pardo, "CH_4 continuous measurements in the upper Spanish plateau," *Environmental Monitoring and Assessment*, vol. 186, no. 5, pp. 2823–2834, 2014.

[7] I. A. Pérez, M. L. Sánchez, M. Á. García, and N. Pardo, "Analysis of CO_2 daily cycle in the low atmosphere at a rural site," *Science of the Total Environment*, vol. 431, no. 1, pp. 286–292, 2012.

[8] Y. K. Tiwari, J. V. Revadekar, and K. Ravi Kumar, "Variations in atmospheric carbon dioxide and its association with rainfall and vegetation over India," *Atmospheric Environment*, vol. 68, pp. 45–51, 2013.

[9] I. A. Pérez, F. Artuso, M. Mahmud, U. Kulshrestha, M. L. Sánchez, and M. A. García, "Applications of air mass trajectories," *Advances in Meteorology*, vol. 2015, Article ID 284213, 20 pages, 2015.

[10] X. Huang, T. Wang, R. Talbot et al., "Temporal characteristics of atmospheric CO_2 in urban Nanjing, China," *Atmospheric Research*, vol. 153, pp. 437–450, 2015.

[11] C. Du, S. Liu, X. Yu et al., "Urban boundary layer height characteristics and relationship with particulate matter mass concentrations in Xi'an, central China," *Aerosol and Air Quality Research*, vol. 13, no. 5, pp. 1598–1607, 2013.

[12] L.-W. Lai, "Fine particulate matter events associated with synoptic weather patterns, long-range transport paths and mixing height in the Taipei Basin, Taiwan," *Atmospheric Environment*, vol. 113, pp. 50–62, 2015.

[13] Y. Wang, Q. Li, S. Wang et al., "Seasonal and diurnal variations of atmospheric PAHs and OCPs in a suburban paddy field, South China: impacts of meteorological parameters and sources," *Atmospheric Environment*, vol. 112, pp. 208–215, 2015.

[14] J. A. Adame, C. Córdoba-Jabonero, M. Sorribas, D. Toledo, and M. Gil-Ojeda, "Atmospheric boundary layer and ozone-aerosol interactions under Saharan intrusions observed during AMISOC summer campaign," *Atmospheric Environment*, vol. 104, pp. 205–216, 2015.

[15] I. A. Pérez, M. L. Sánchez, and M. Á. García, "CO_2 dilution in the lower atmosphere from temperature and wind speed profiles," *Theoretical and Applied Climatology*, vol. 107, no. 1-2, pp. 247–253, 2012.

[16] I. Levy, U. Dayan, and Y. Mahrer, "Differing atmospheric scales of motion and their impact on air pollutants," *International Journal of Climatology*, vol. 30, no. 4, pp. 612–619, 2010.

[17] G. Surkova, "Air recirculation and ventilation in the coastal regions of the Black Sea," *Open Geosciences*, vol. 5, no. 2, pp. 196–207, 2013.

[18] D. K. Papanastasiou and D. Melas, "Climatology and impact on air quality of sea breeze in an urban coastal environment," *International Journal of Climatology*, vol. 29, no. 2, pp. 305–315, 2009.

[19] I. A. Pérez, M. L. Sánchez, M. Á. García, and V. Paredes, "Relationship between CO_2 at a rural site and integral measures of atmospheric stagnation, recirculation, and ventilation," *Naturwissenschaften*, vol. 98, no. 7, pp. 565–574, 2011.

[20] K. J. Allwine and C. D. Whiteman, "Single-station integral measures of atmospheric stagnation, recirculation and ventilation," *Atmospheric Environment*, vol. 28, no. 4, pp. 713–721, 1994.

[21] I. A. Pérez, M. L. Sánchez, M. Á. García, and N. Pardo, "Spatial analysis of CO_2 concentration in an unpolluted environment in northern Spain," *Journal of Environmental Management*, vol. 113, pp. 417–425, 2012.

[22] N. Pérez, G. Rodríguez, and J. M. Pacheco, "Atmospheric recirculation on the east coast of Gran Canaria Island," in *Proceedings of Air Pollution XXII*, vol. 183, pp. 15–25, WIT Transactions on Ecology Environment, Opatija, Croatia, July 2014.

[23] A. Karagiannidis, A. Poupkou, T. Giannaros, C. Giannaros, D. Melas, and A. Argiriou, "The air quality of a Mediterranean urban environment area and its relation to major meteorological parameters," *Water, Air and Soil Pollution*, vol. 226, no. 1, article 2239, 2015.

[24] I. A. Pérez, M. L. Sánchez, M. Á. García, and B. de Torre, "CO_2 transport by urban plumes in the upper Spanish plateau,"

Science of the Total Environment, vol. 407, no. 17, pp. 4934–4938, 2009.

[25] L. L. Ashbaugh, W. C. Malm, and W. Z. Sadeh, "A residence time probability analysis of sulfur concentrations at Grand Canyon National Park," *Atmospheric Environment (1967)*, vol. 19, no. 8, pp. 1263–1270, 1985.

[26] I. A. Pérez, M. L. Sánchez, M. Á. García, and V. Paredes, "Directional analysis of CO_2 persistence at a rural site," *Science of the Total Environment*, vol. 409, no. 19, pp. 3887–3893, 2011.

[27] A. Donnelly, B. Misstear, and B. Broderick, "Application of nonparametric regression methods to study the relationship between NO_2 concentrations and local wind direction and speed at background sites," *Science of the Total Environment*, vol. 409, no. 6, pp. 1134–1144, 2011.

[28] M. Á. García, M. L. Sánchez, and I. A. Pérez, "Differences between carbon dioxide levels over suburban and rural sites in Northern Spain," *Environmental Science and Pollution Research*, vol. 19, no. 2, pp. 432–439, 2012.

[29] I. A. Pérez, M. L. Sánchez, M. Á. García, and N. Pardo, "Features of the annual evolution of CO_2 and CH_4 in the atmosphere of a Mediterranean climate site studied using a nonparametric and a harmonic function," *Atmospheric Pollution Research*, vol. 7, no. 6, pp. 1013–1021, 2016.

[30] J. Zeng, T. Matsunaga, and H. Mukai, "METEX—a flexible tool for air trajectory calculation," *Environmental Modelling & Software*, vol. 25, no. 4, pp. 607-608, 2010.

[31] NASA, "Earth observing system data and information system," 2018, https://earthdata.nasa.gov/.

[32] Ministerio de Fomento, "National geographic Institute," 2018, http://www.fomento.gob.es/.

[33] R. C. Henry, Y.-S. Chang, and C. H. Spiegelman, "Locating nearby sources of air pollution by nonparametric regression of atmospheric concentrations on wind direction," *Atmospheric Environment*, vol. 36, no. 13, pp. 2237–2244, 2002.

[34] B. W. Silverman, *Density Estimation for Statistics and Data Analysis*, Chapman & Hall/CRC, Boca Raton, FL, USA, 1998.

[35] J. P. Snyder, *Map Projections—A Working Manual*, U.S. Government Printing Office, Washington, DC, USA, 1987.

[36] ICGC, "Mapping and Geological Institute of Catalonia," 2018, http://www.icgc.cat/.

[37] M. Á. García, M. L. Sánchez, I. A. Pérez, M. I. Ozores, and N. Pardo, "Influence of atmospheric stability and transport on CH_4 concentrations in northern Spain," *Science of the Total Environment*, vol. 550, pp. 157–166, 2016.

[38] N. Kolev, P. Savov, E. Donev et al., "Boundary layer development and meteorological parameters impact on the ground level ozone concentration over an urban area in a mountain valley (Sofia, Bulgaria)," *International Journal of Remote Sensing*, vol. 32, no. 24, pp. 8915–8933, 2011.

[39] S. Pal, M. Lopez, M. Schmidt et al., "Investigation of the atmospheric boundary layer depth variability and its impact on the ^{222}Rn concentration at a rural site in France," *Journal of Geophysical Research: Atmospheres*, vol. 120, no. 2, pp. 623–643, 2015.

[40] G. Sreenivas, P. Mahesh, J. Subin, A. L. Kanchana, P. V. N. Rao, and V. K. Dadhwal, "Influence of Meteorology and interrelationship with greenhouse gases (CO_2 and CH_4) at a suburban site of India," *Atmospheric Chemistry and Physics*, vol. 16, no. 6, pp. 3953–3967, 2016.

[41] A. Russo, C. Gouveia, I. Levy et al., "Coastal recirculation potential affecting air pollutants in Portugal: the role of circulation weather types," *Atmospheric Environment*, vol. 135, pp. 9–19, 2016.

[42] D. Kumar, A. Kumar, V. Kumar, J. Kumar, and P. M. Ravi, "Study of atmospheric stagnation, recirculation and ventilation potential at Narora Atomic Power Station NPP site," *Environmental Monitoring and Assessment*, vol. 185, no. 4, pp. 2887–2894, 2013.

[43] L. E. Venegas and N. A. Mazzeo, "Atmospheric stagnation, recirculation and ventilation potential of several sites in Argentina," *Atmospheric Research*, vol. 52, no. 1-2, pp. 43–57, 1999.

[44] D. P. Nankar, A. K. Patra, M. U. Dole, S. Venkataraman, and A. G. Hegde, "Atmospheric stagnation, recirculation and ventilation characteristics at Kakrapar atomic power station site," *Annals of Nuclear Energy*, vol. 36, no. 4, pp. 475–480, 2009.

[45] E. H. Kim, K. S. Suh, W. T. Hwang, H. J. Jeong, M. H. Han, and J. Y. Moon, "Analysis of the site characteristics of Korean nuclear power sites from the meteorological aspects," *Annals of Nuclear Energy*, vol. 34, no. 9, pp. 719–723, 2007.

[46] Y. Charabi and S. Al-Yahyai, "Integral assessment of air pollution dispersion regimes in the main industrialized and urban areas in Oman," *Arabian Journal of Geosciences*, vol. 4, no. 3-4, pp. 625–634, 2011.

[47] I. Levy, U. Dayan, and Y. Mahrer, "A five-year study of coastal recirculation and its effect on air pollutants over the East Mediterranean region," *Journal of Geophysical Research Atmospheres*, vol. 113, no. 16, article D16121, 2008.

[48] I. A. Pérez, M. L. Sánchez, M. Á. García, and N. Pardo, "Analysis of air mass trajectories in the northern plateau of the Iberian Peninsula," *Journal of Atmospheric and Solar-Terrestrial Physics*, vol. 134, pp. 9–21, 2015.

[49] R. Lorente-Plazas, J. P. Montávez, P. A. Jimenez et al., "Characterization of surface winds over the Iberian Peninsula," *International Journal of Climatology*, vol. 35, no. 6, pp. 1007–1026, 2015.